



Evaluation and Modification of a Robust Path Following Controller for Marine Surface Vessels in Wave Fields

Journal:	<i>Journal of Ship Research</i>
Manuscript ID:	JSR-12-08-0045.R1
Manuscript Type:	Original Article
Date Submitted by the Author:	01-Apr-2009
Complete List of Authors:	Li, Zhen; University of Michigan, Naval Architecture and Marine Engineering Sun, Jing; University of Michigan, Naval Architecture and Marine Engineering Beck, Robert; University of Michigan, Naval Architecture and Marine Engineering
Keywords:	navigation, maneuvering, waves



Evaluation and Modification of a Robust Path Following Controller for Marine Surface Vessels in Wave Fields

Zhen Li, Jing Sun and Robert F. Beck

Department of Naval Architecture and Marine Engineering, University of Michigan, Ann Arbor, USA

This paper evaluates a novel robust path following controller for marine surface vessels in wave fields. Due to complex wave structure interactions, most path following control designs neglect the wave impact at the design stage, and rely on simulation or experiment to assure the satisfactory performance in wave fields. In this paper, we first introduce a numerical test-bed that combines the ship dynamics and wave effects on vessels to facilitate the model-base performance evaluation of path following control systems in wave fields. Then, a novel robust path following controller is described and its key features are summarized. Simulation results of the path following controller in the wave field are presented. Several issues, such as steady state errors and rudder oscillations, have been identified, thereby motivating controller modification and gain re-tuning. Mitigating strategies for improving the controller performance are proposed and numerically evaluated. The simulation results show that the performance of the modified controller can be substantially improved in wave fields.

Key Words: Ship control, Path Following, Wave fields, Marine surface vessels

1. Introduction

PATH following or trajectory tracking are two important marine control problems that have attracted considerable interests, leading to many publications on the subject (Breivik and Fossen 2004a, Breivik and Fossen 2004b, Do et al. 2002, Do and Pan 2003, Do et al. 2004, Do and Pan 2006, Encarnacao and Pascoal 2001, Fossen et al. 2003, Jiang 2002, Lefeber et al. 2003, Li et al. 2007, Pettersen and Nijmeijer 1998, Pettersen and Lefeber 2001, Skjetne and Fossen 2001, Skjetne et al. 2004). With a few exceptions, most of the designs reported in the literature assume calm water operation without accounting for the wave influence on the vessels. In the work of (Breivik and Fossen 2004a, Breivik and Fossen 2004b), the wave effects, together with wind and current effects, are approximated by constant loads in the control design, leading to wave load terms in the control laws. Given that the wave loads can not be measured in a seaway, the implementation of such controllers requires an estimation algorithm for the wave load.

Given the stringent safety and performance requirements for both military and commercial ships and the cost associated with the testing and operation of vessels, detailed models that capture wave-ship interactions can be a great asset in the numerical evaluation of path following and trajectory tracking control system performance in a seaway. Recently, Perez et al. (2006) presents a valuable 1st order wave excitation force calculation program using force frequency response functions (FRF). While such a model provides credible wave excitation loads, the second order drift loads are not included. However, the second order wave loads are of importance in several contexts for marine systems such as added ship resistance and drift effects (Faltinsen 1990).

Motivated by these issues, this paper presents a test-bed, which combines the ship dynamics and the wave force calculations (both first order excitation and second order drift forces), to evaluate the performance of ship motion control systems such as path following, course keeping, roll stabilization etc. The test-bed is then used to evaluate a novel robust path following controller, which was developed and analyzed recently (Li et al. 2007) for calm water. Several issues, such as steady state errors and rudder oscillations are observed through numerical simulations. To address these problems, modifications are made by proper gain tuning to improve the controller performance. The simulation results show that the modified controller maintains the desired performance in wave fields.

This paper is organized as follows: in Section 2, a numerical test-bed combining ship dynamics and wave force calculation is presented. The path following controller design and analysis are summarized in Section 3. In Section 4, the path following controller is evaluated in the wave fields. The modification of the controller is presented in Section 5, followed by the conclusions in Section 6.

2. A Numerical Test-bed for Ship's Maneuvering in a Seaway

In this section, we introduce a 4 DoF nonlinear container model and present a wave load calculation program, which incorporates both the 1st and 2nd order wave forces and moments acting on the vessel.

2.1 Marine Surface Vessel Model

A mathematical model for a single-screw high-speed container ship in surge, sway, roll and yaw has been presented in (Fossen 1994). This 4-DoF nonlinear ship dynamical model has 10 states and 2 control inputs: $\underline{X} = [u, v, r, p, \eta_1, \eta_2, \psi, \phi, n, \delta]$ and $U = [n_c, \delta_c]$. The variables u, v, r and p are the surge velocity, sway velocity, yaw rate and roll rate with respect to the ship-fixed frame respectively, the corresponding displacements with respect to the inertial frame are denoted as η_1, η_2, ψ and ϕ . The dynamics of the propeller shaft speed n and rudder angle δ are captured by first order systems, with n_c and δ_c , the commands for the propeller speed and rudder angle respectively as their inputs. The actuator input saturation and rate limits are also incorporated in this model. The nonlinear equations of motion (surge u , sway v , roll p and yaw r) are given by:

$$(m + m_x)\dot{u} - (m + m_y)vr = X, \quad (1)$$

$$(m + m_y)\dot{v} + (m + m_x)ur + m_y\alpha_y\dot{r} - m_y l_y \dot{p} = Y, \quad (2)$$

$$(I_x + J_x)\dot{p} - m_y l_y \dot{v} - m_x l_x ur + WGM\dot{\phi} = K, \quad (3)$$

$$(I_z + J_z)\dot{r} + m_y\alpha_y\dot{v} = N - Yx_G. \quad (4)$$

Here, m denotes the ship mass, m_x and m_y denote the added mass in the x and y directions respectively. I_x and I_z denote the moment of inertia and J_x and J_z denote the added moment of inertia about the x and z axes, respectively. Please note that the added mass and moment of inertia are excitation frequency dependent. However, they are normally assumed as constants in the maneuvering model since the vessel is operated in the low frequency range. Furthermore, α_y denotes the x -coordinate of the center of m_y , and l_x and l_y , the z -coordinates of the centers of m_x and m_y respectively. W is the ship displacement, GM is the vertical distance between the center of gravity and the metacenter and x_G is the location of the center of gravity in x -axis (for this particular container, $x_G = 0$). The readers are referred to (Fossen, 1994) for the details of the hydrodynamic forces and moments, namely X, Y, K and N , and the propeller and rudder dynamics.

The 4-DoF nonlinear model is one of the most comprehensive ship models presented in open literature. It captures the fundamental characteristics of the ship dynamics and offers satisfactory accuracy over a wide range of operating conditions in open-loop simulations. However, the model is based on the calm water assumption and does not include the interaction between the vessel and waves. Wave loads, reflecting the induced forces acting on the ship due to structure-wave interactions, lead to additional terms to the right-hand side of the dynamical equations. The following sub-section is devoted to the calculation of the first and second order wave loads to develop a model that captures the dynamic behavior of the ship in the wave field.

2.2 Wave Load Calculations

The coordinate system used in the wave force calculation is shown in Fig. 1. β , the ship heading angle with respect to the wave heading angle, is defined as:

$$\beta = \theta_{wave} - \theta_{ship}, \quad (5)$$

where θ_{wave} and θ_{ship} are the wave heading angle and ship heading angle in the earth fixed frame respectively.

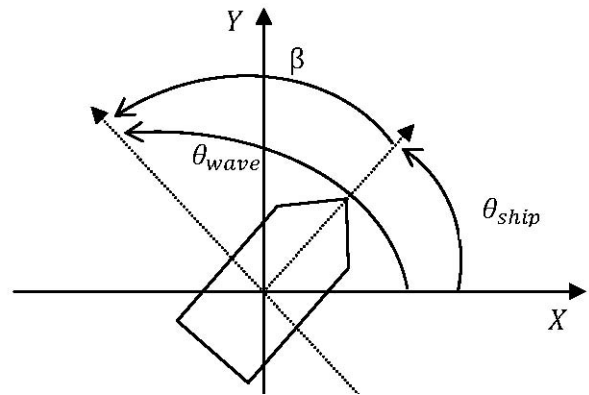


Figure 1. Angle definitions.

- 1st Order Wave Excitation Force and Moment

The calculation of the 1st-order wave excitation forces is very involved. An irregular sea (Lewis, 1989) surface can be expressed as a sum of single frequency waves with different frequencies (ω_i), wavenumbers (\underline{k}_i), and uniformly distributed random phase angles (α_i):

$$\eta(x, t) = \sum_{i=1}^N A_i \cos(\omega_i t - \underline{k}_i \underline{x} + \alpha_i), \quad (6)$$

where A_i is the corresponding wave amplitude and \underline{x} is the position vector.

By linear seakeeping theory (Lewis, 1989), the wave excitation forces and moments can be expressed by the following equations:

$$f_j(\underline{x}, t) = \sum_{i=1}^N A_i |H_j(\omega_i, \beta, u)| \cos(\omega_i t - \underline{k}_i \underline{x} + \alpha_i + \delta_j(\omega_i, \beta, u)), \quad (7)$$

for directional index $j = 1, 2, 3, 4, 5, 6$, which stand for surge, sway, heave, roll, pitch and yaw respectively. $H_j(\omega, \beta, u)$ is the response amplitude operator (RAO) in the j direction, with a magnitude $|H_j(\omega, \beta, u)|$ and a phase angle $\delta_j(\omega, \beta, u)$. By definition, the RAO (such as $H_j(\omega, \beta, u)$) is the response of the ship system, such as the ship motion variable, wave forces, per wave height due to a wave of frequency ω , a wave heading β and ship speed u (Lewis, 1989). For our purpose, only the index 1, 2, 4 and 6 are used for surge, sway forces and roll, yaw moments respectively. More details on the calculation of the RAO can be found in (Wolfe, 2007).

In the calculation of first order wave loads, a quasi-steady approach is adopted where the transient effects are neglected in order to greatly simplify the computation, because the calculation of transients involves computational convolution integrals. The similar approach is employed in (Perez et al. 2006).

- 2st Order Wave Drift Force and Moment

For the wave-induced drift force in the surge direction (\bar{f}_1), we approximate the 2nd-order drift forces by an empirical equation (Dolinskaya et al., 2008) which is a sixth order polynomial function of forward speed u (m/s) and relative ship heading angle β (rad):

$$\begin{aligned} \bar{f}_1 = & C_0 + C_{10}u + C_{01}\beta + C_{20}u^2 + C_{11}u\beta + C_{02}\beta^2 \\ & + C_{21}u^2\beta + C_{12}u\beta^2 + C_{03}\beta^3 + C_{22}u^2\beta^2 \\ & + C_{13}u\beta^3 + C_{04}\beta^4 + C_{23}u^2\beta^3 + C_{14}u\beta^4 \\ & + C_{24}u^2\beta^4, \end{aligned} \quad (8)$$

where $C_0, C_{10}, C_{01}, C_{20}, C_{11}, C_{02}, C_{21}, C_{12}, C_{03}, C_{22}, C_{13}, C_{04}, C_{23}, C_{14}$ and C_{24} are the empirical coefficients fitted using data generated from detailed ship numerical simulation program (see (Dolinskaya et al., 2008) for the details). For the container ship S175 in sea state 5 (corresponding to 3.25 m of significant wave height), the above coefficients are summarized in Table 1.

Table 1. Empirical coefficients for calculation of second order drift wave force in surge

C_0	C_{10}	C_{01}	C_{20}	C_{11}
84.988	32.040	-487.122	-2.436	40.734
C_{02}	C_{21}	C_{12}	C_{03}	C_{22}
1076.446	-0.348	-135.610	-577.089	5.582
C_{13}	C_{04}	C_{23}	C_{14}	C_{24}
77.390	91.061	-3.558	-12.646	0.606

For the drift sway force and the drift yaw moment, the following empirical equations were developed in (Daidola, 1986):

$$\bar{f}'_2 = \frac{1}{2} \rho g L \zeta^2 \sin \beta C_Y, \quad (9)$$

$$\bar{f}'_6 = \frac{1}{2} \rho g L^2 \zeta^2 \sin \beta C_N, \quad (10)$$

where ρ is the water density, g is the acceleration due to gravity, L is the ship length, ζ is the mean wave amplitude, C_Y and C_N are the corresponding empirical coefficients, whose expressions are given as follows:

$$C_Y = 0.46 + 6.83 \frac{\lambda}{L} - 11.65 \left(\frac{\lambda}{L} \right)^2 + 8.44 \left(\frac{\lambda}{L} \right)^3, \quad (11)$$

$$C_N = 0.11 + 0.68 \frac{\lambda}{L} - 0.79 \left(\frac{\lambda}{L} \right)^2 + 0.21 \left(\frac{\lambda}{L} \right)^3, \quad (12)$$

where λ is the mean wave length. However, (11) and (12) are regressed from the data of the specific ship with zero speed in (English and Wise, 1975). For different ships with nonzero speed, these two coefficients need to be corrected. We introduce speed dependent coefficients $C_{f2}(u)$ and $C_{f6}(u)$ to correct the second order drift loads by the following equations:

$$\bar{f}'_2 = C_{f2}(u) \bar{f}'_2, \quad (13)$$

$$\bar{f}'_6 = C_{f6}(u) \bar{f}'_6. \quad (14)$$

It was pointed out in (Faltinsen, 1990) that the ratio between the magnitudes of the mean wave drift forces and linear first-order wave forces is about $\zeta/100$. For different speeds, the coefficients $C_{f2}(u)$ and $C_{f6}(u)$ adopted in this paper are calculated using the magnitude of the 1st order excitation loads, which are calculated based on the detailed information of the ship hull form using the linear seakeeping theory. More specifically, given the vessel speed and mean wave amplitude ζ , we first calculate the mean amplitudes of the first order wave loads in sway and yaw, namely F_{f2} and F_{f6} , for β equal to 45, 90 and 135 deg. Then the correction coefficients $C_{f2}(u)$ and $C_{f6}(u)$ are obtained by averaging the corresponding three values of $F_{f2}\zeta/(100|f'_2|)$ and $F_{f6}\zeta/(100|f'_6|)$. In this paper, for the container ship S175 with a speed of 10 m/s in sea state 5, the values of $C_{f2}(u)$ and $C_{f6}(u)$ are 0.2535 and 0.5211 respectively.

2.3 Integrated Ship Dynamics and Wave Load Model

The forces/moments X, Y, K and N that appear in the system (1)-(4) are the calm water hydrodynamic forces and moments. In an incident wave field, the following modifications should be adopted:

$$X_w = X + \bar{f}_1 + \bar{f}'_1, \quad (15)$$

$$Y_w = Y + \bar{f}_2 + \bar{f}'_2, \quad (16)$$

$$K_w = K + \bar{f}_4, \quad (17)$$

$$N_w = N + \bar{f}_6 + \bar{f}'_6, \quad (18)$$

where X_w, Y_w, K_w and N_w are corresponding hydrodynamic forces and moments in the incident wave field and will replace X, Y, K and N in the equations (1)-(4) when waves exist. As mentioned in sub-section 2.2, $\bar{f}_1, \bar{f}_2, \bar{f}_4$ and \bar{f}_6 are the corresponding first order wave loads and \bar{f}'_1, \bar{f}'_2 and \bar{f}'_6 are the corresponding second order wave loads. Note that the second order moment in roll is neglected. Using (15)-(18) in (1)-(4), the wave induced loads are incorporated into the ship dynamics, with the assumption that the damping and added mass of the ship are unchanged in the wave field.

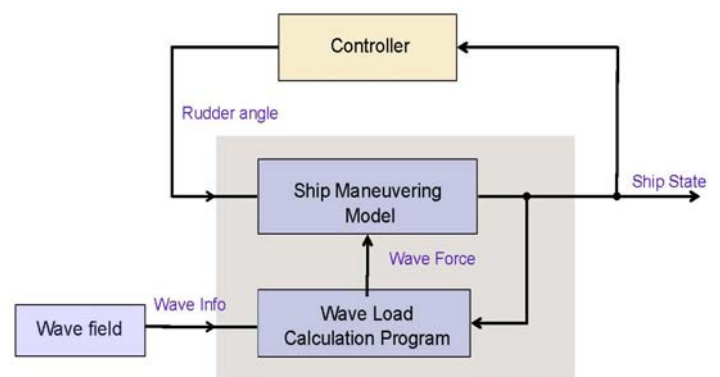


Figure 2. Block diagram of the simulation model.

Fig. 2 shows the block diagram of the overall model. The wave load program calculates the wave induced forces and moments based on the wave field information (sea state, dominant wave direction) and the ship states (position, heading and speed). The ship maneuvering model is driven by the wave forces and moments, together with the control input (rudder angle calculated based on a control law using the current ship state measurement or estimation).

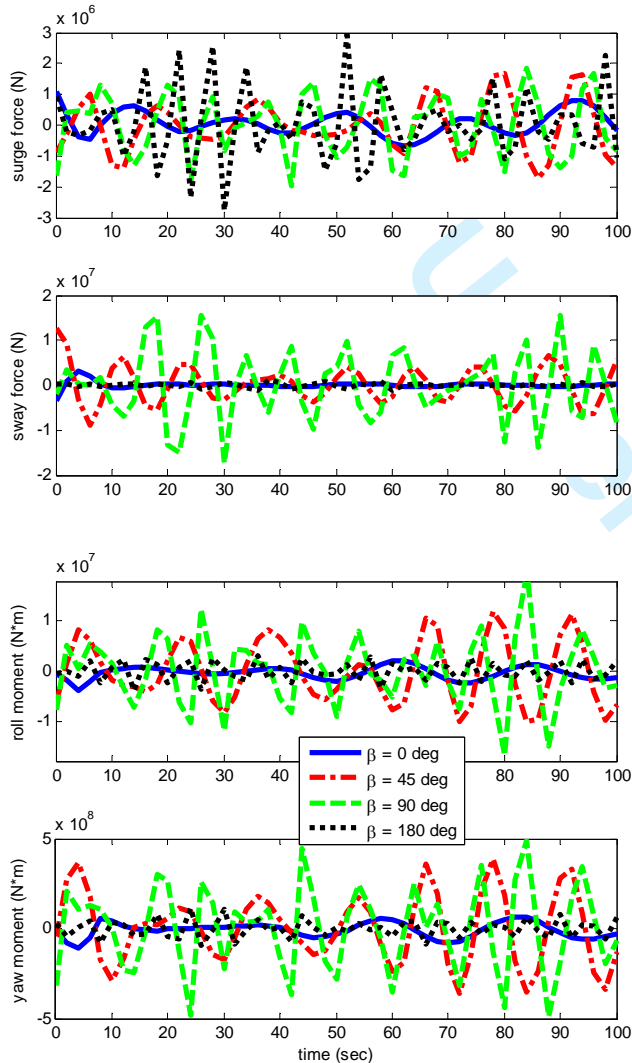


Figure 3. First order wave excitation forces and moments with different wave heading angles.

As an example, Fig. 3 shows the wave-induced first order excitation forces and moment for four different heading angles, namely following sea ($\beta = 0$ deg), quartering sea ($\beta = 45$ deg), beam sea ($\beta = 90$ deg) and head sea ($\beta = 180$ deg). In simulations, the JONSWAP spectrum (Faltinsen, 1990) was adopted with 3.25 m significant wave height (sea state 5), 9.53 sec peak period and default Gamma peak factor 3.3. The ship

used in the simulation is a container ship S175, which is widely used in research and described in (Fossen, 1994). The ship velocity is maintained at 10 m/sec. From Fig. 3, we can see that the wave load calculation program captures the key characteristics of the wave excitation loads on vessels in a short crested wave field. For example, the head sea has the highest encounter frequency while the following has the lowest frequency; the beam sea has the largest sway force and roll moment among these four cases while these loads are relatively small in the following sea and head sea cases; the head sea has the largest surge force and the following sea and head sea have very small sway force.

In this paper, we use the proposed numerical test-bed to evaluate the path following controller. This numerical test-bed is established in MATLAB, which is the most popular software in the control community. The program calculating the first order wave induced loads is coded in FORTRAN and called from the main program in MATLAB for the computational efficiency.

It should be pointed out that this model is generic and can be used in many other applications, such as course keeping, roll stabilization and dynamical positioning. For example, the vessel motion controllers in (Parsons et al. 1995, Cao et al. 2000 and Cao and Lee 2003) can also use this numerical test-bed to evaluate the controller performance in the wave fields.

3. Introduction of a Robust Path Following Controller

In our previous work (Li et al., 2007), a robust path following controller was designed based on the reduced order linear model without wave loads, which was derived from the calm water 10th order nonlinear ship model (1)-(4). The controller uses the rudder as the control input, and treats the propeller speed as a constant which is regulated by an independent control system. Using back-stepping (Krstic et al., 1995) together with the feedback dominance technique, the following controller was developed:

$$\delta = -\frac{1}{b_2} \left[(c_1 c_2 c_3 + \frac{1}{c_1 p_2}) e + (c_2 c_3 + \frac{1}{c_1^2 p_2}) \bar{\psi} \right] + (a_{22} + c_2 + c_3) r + c_1 c_2 u \sin \bar{\psi}, \quad (19)$$

where c_1 , c_2 , c_3 and p_2 are positive controller gains, a_{22} and b_2 are constant ship parameters. e , the cross-track error, and $\bar{\psi}$, the heading error have the dynamics of (20) and (21).

The controller has two advantages: 1) it is simple and easy to calibrate compared with other backstepping controllers reported in the literature (Do et al., 2002; Do and Pan, 2003; Do et al., 2004; Encarnacao and Pascoal, 2001; Fossen et al., 2003; Lapiere et al., 2003; Pettersen and Nijmeijer, 1998; Skjetne and Fossen, 2001; Skjetne et al., 2004). Note that the controller (19) has the proportional, integral and derivative terms when e and r are expressed in terms of $\bar{\psi}$, the tuning of the controller gains are relatively easy in the sense that the effects of each parameter on the system dynamics and control saturation can be interpreted in physical variables and many of the PID tuning algorithms can be used. 2) It is robust with respect to model uncertainties. While the design was based on a simplified ship

model with sway dynamics ignored, the effects of the nonlinearities are included as unmodeled dynamics and the sway dynamics are incorporated in the control performance evaluation. Through rigorous Lyapunov analysis, we have shown that the control system is indeed robust with respect to unmodeled dynamics, and the error for the cross-track distance and heading can be contained within a neighborhood around the origin. More importantly, the errors can be made arbitrarily small by properly selecting the controller gains. The results are documented in a journal paper recently accepted by Automatica (Li et al., 2009).

4. Controller Evaluation in Wave Fields

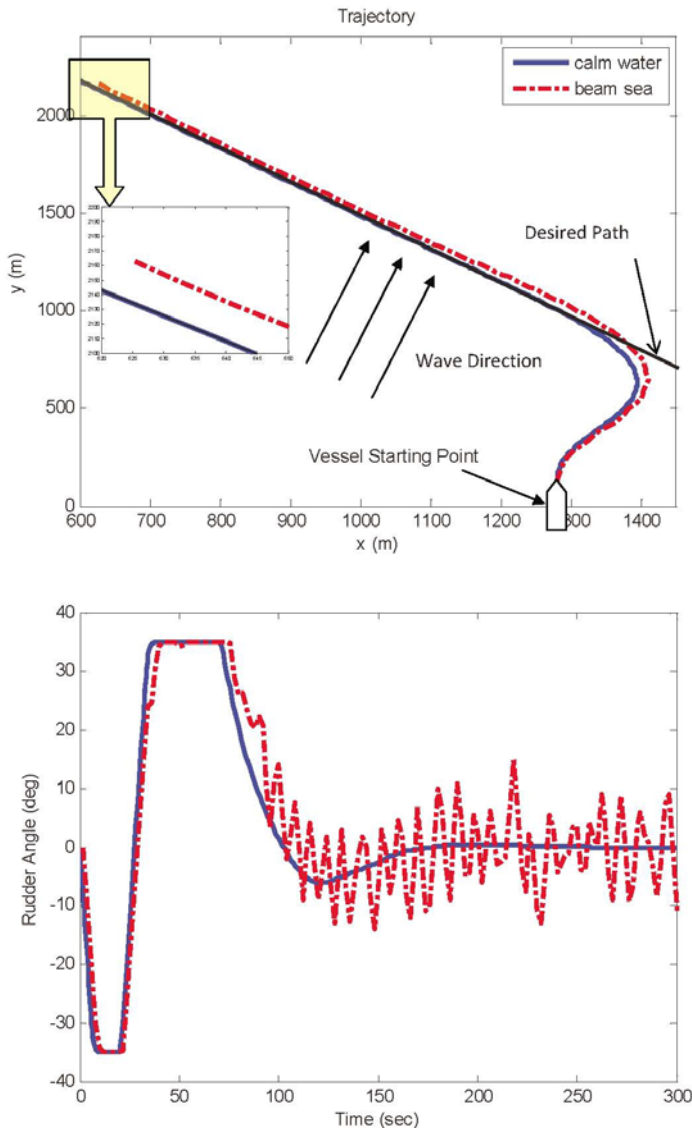


Figure 4. Simulation results of the ship response in beam sea and calm water with gain set 1.

The proposed robust path following controller, developed based on the reduced order linear ship model in calm water, is

implemented and simulated with the full order original model incorporating the wave effects to evaluate the performance. The actuator saturation and its rate limits ($|\delta| \leq 35$ deg and $|\dot{\delta}| \leq 5$ deg/sec) are also incorporated in the evaluations. In the simulation, $u = 10$ m/s, $a_{22} = -0.10676$, $b_2 = 0.0028385$ and the propeller speed is maintained as constant (99.50 RPM).

We choose the controller gain to be: $c_1 = 0.0033$, $c_2 = 0.1$, $c_3 = 0.1$, $p_2 = 10^{11}$ (this gain set is named gain set 1 in the subsequent discussions). Note that the scales of e , $\bar{\psi}$ and r are very different, with e having values of order of magnitude larger than $\bar{\psi}$ and r . The large value of p_2 is employed to normalize the effects of different states in the Lyapunov function, as detailed in (Li et al., 2009). The value of c_1 , c_2 , and c_3 are tuned to achieve good closed-loop path following performance in calm water. The effects of the waves on the dynamic response of the controller are first illustrated in Fig. 4, compared with the calm water case. The beam sea is used in the simulation since it normally introduces the largest motions in sway and roll. The significant wave height in the simulations is 3.25 m (sea state 5) and it will be kept the same in all other simulations.

From Fig. 4, we can see that the waves do have an impact on the container ship's response. The proposed path following controller achieves the path following with a steady state error. The wave force pushes the vessel off the desired trajectory. Furthermore, the undesired oscillations in rudder response can be observed from Fig. 4.

The steady state error in the path following and rudder oscillations were also reported in the simulation results of a fuzzy controller in (Vukic et al., 1998), where there exist the external disturbances from a passing ship or sea current. They solved this problem by introducing an adaptive fuzzy controller (Velagic et al., 2000). However, neither of these two papers could eliminate the rudder oscillations. The rudder oscillations in the course-keeping stage cause wear and tear of the steering gear, efforts have been reported in the literature to reduce or eliminate their impacts. Typical mitigating solutions include low gains, dead zone or rudder limits and filtering of the signals (Amerongen and van Nauta Lemke, 1978, 1980). It should be pointed out that each solution has its associated limitations. For example, the low gain has to compromise fast course changing for good course keeping, while the dead zone might lead to sluggish course steering. On the other hand, the effectiveness of the filtering depends on a good knowledge of the cut-off frequency, whose estimation will further complicate the overall control system.

5. Controller Modification

To search for an alternative solution to mitigate the problems for the path following control in the seaway, we analyze the wave impacts on the controller performance and identify the reasons for the steady state error and rudder oscillations.

Steady state error is largely due to the second order drift force, which results in a non-zero equilibrium point if the controller gains are not properly selected. We use the simplified vessel model to analyze the reason of the steady state error.

When the waves exist, the overall system dynamics can be described as follows:

$$\dot{e} = u \sin \bar{\psi} + v \cos \bar{\psi}, \quad (20)$$

$$\dot{\bar{\psi}} = r, \quad (21)$$

$$\dot{v} = a_{11}v + a_{12}r + b_1\delta + \frac{m_{66}(\bar{f}_2 + f_2) - m_{62}(\bar{f}_6 + f_6)}{m_{22}m_{66} - m_{62}^2}, \quad (22)$$

$$\dot{r} = a_{21}v + a_{22}r + b_2\delta + \frac{m_{22}(\bar{f}_6 + f_6) - m_{62}(\bar{f}_2 + f_2)}{m_{22}m_{66} - m_{62}^2}, \quad (23)$$

where (20) and (21) are the original path following error dynamics. The equation (22) and (23) are the 2 DoF linearized vessel model with wave loads. Moreover, a_{11} , a_{12} , a_{21} , a_{22} , b_1 and b_2 are constant ship parameters, $m_{22} = m + m_y$, $m_{66} = I_z + J_z$ and $m_{62} = m_y a_y$.

The equilibrium point of the overall system (20)-(23) is the solution of the equations:

$$u \sin \bar{\psi} + v \cos \bar{\psi} = 0, \quad (24)$$

$$a_{11}v + b_1\delta + \frac{m_{66}\bar{f}_2 - m_{62}\bar{f}_6}{m_{22}m_{66} - m_{62}^2} = 0, \quad (25)$$

$$a_{21}v + b_2\delta + \frac{m_{22}\bar{f}_6 - m_{62}\bar{f}_2}{m_{22}m_{66} - m_{62}^2} = 0. \quad (26)$$

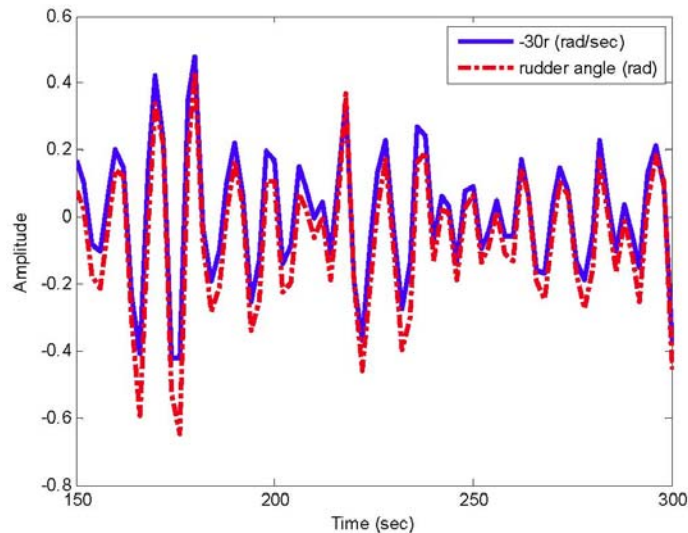


Figure 5. The state histories in wave fields (gain set 1).

Notice that $r = 0$ and the zero-mean oscillating 1st order wave loads are neglected since they do not affect the equilibrium position. According to the control law (19), δ is a function of e and $\bar{\psi}$. Therefore, the above three equations (24)-(26) have three unknowns, namely v , e and $\bar{\psi}$. And the solution of these three equations depends on the controller gains c_1 , c_2 , c_3 and p_2 . If gain set 1 is selected, the steady state error given by the (24)-(26) is $e_0 = -16.67$ (m), $\bar{\psi}_0 = 4.6$ (deg) and $v_0 = -0.64$ (m/s), which match the simulation result given in Fig. 4. To reduce or eliminate the steady state error, the gains c_1 , c_2 , c_3 and p_2 should

be properly selected. The proper gains that eliminate the steady state error should satisfy the following two equations:

$$a_{11}v_0 - \frac{b_1}{b_2} \left[(c_2c_3 + \frac{1}{c_1^2 p_2}) \bar{\psi}_0 + c_1c_2u \sin \bar{\psi}_0 \right] + \frac{m_{66}\bar{f}_2 - m_{62}\bar{f}_6}{m_{22}m_{66} - m_{62}^2} = 0, \quad (27)$$

$$a_{21}v_0 - (c_2c_3 + \frac{1}{c_1^2 p_2}) \bar{\psi}_0 - c_1c_2u \sin \bar{\psi}_0 + \frac{m_{22}\bar{f}_6 - m_{62}\bar{f}_2}{m_{22}m_{66} - m_{62}^2} = 0. \quad (28)$$

Notice that e_0 is set to zero to derive (27)-(28) from (24)-(26). To solve (27)-(28), let $\bar{\psi}_0 = 4.6$ (deg) and $v_0 = -0.64$ (m/s), which is the same as the solution of gain set 1. For a given wave field with a specific sea state, the steady state errors in the heading error and sway velocity should be the same to counteract the same wave drift loads, regardless of the controller gains.

The reason for the rudder oscillations is the state oscillations induced by the first order wave excitation load, especially the yaw rate r . The correlation between the rudder angle and yaw rate can be clearly seen in Fig. 5. One intuitive solution to reduce the rudder oscillations is to use the low gain corresponding to the yaw rate term to make the controller insensitive to the oscillating state. More specifically, proper c_2 and c_3 should be selected to make $(a_{22} + c_2 + c_3)$, the coefficient of the r term in control law, small.

From the above analysis, the gain set 2, which corresponds to $c_1 = 0.0023$, $c_2 = 0.05$, $c_3 = 0.05676$ and $p_2 = 10^{11}$ satisfies these two requirements for small or no steady state error in cross-tracking error and rudder oscillations. However, the path following performance of gain set 2 is not satisfactory in the sense that sluggish path following convergence speed is observed in simulation, as shown in Fig. 6. To achieve good path following performance while maintaining small steady state error and rudder oscillations, we propose a gain scheduling approach: 1), if the cross-tracking error is larger than 20m, gain set 1 is adopted for good path following performance and 2), otherwise gain set 2 is employed to have small steady state error in cross-tracking error and rudder oscillations. Because the gains are switched when the cross-tracking is small, which results in small rudder angle, the large rudder angle jump will not happen. The simulation results of modified controller with gain scheduling compared with the original controller are summarized in Fig. 6. From Fig. 6, we can see that the steady state error in path following cross-track error and the rudder oscillations are reduced to an acceptable level without compromising the path following convergent speed.

The proposed path following gain scheduling controller has the great advantage of easy re-tuning to address the environmental disturbance because of its simple form. Furthermore, since no adaptation mechanism and signal filters are adopted in the gain scheduling controller, the complexity of the control system can be largely reduced.

6. Conclusions

In this paper, we evaluated a novel robust path following controller for marine surface vessels in wave fields. A test-bed with ship dynamics and the wave load calculations was first introduced. Such a test-bed is an essential tool that can be used in many applications of ship motion control. Since the steady state error and the rudder oscillations were observed in the evaluation, controller tuning was performed to modify the system response to reduce the steady state cross-track error and rudder oscillations. The simulation validated that the recalibrated controller with gain scheduling achieved satisfactory performance in terms of both path following convergence speed and steady state behavior.

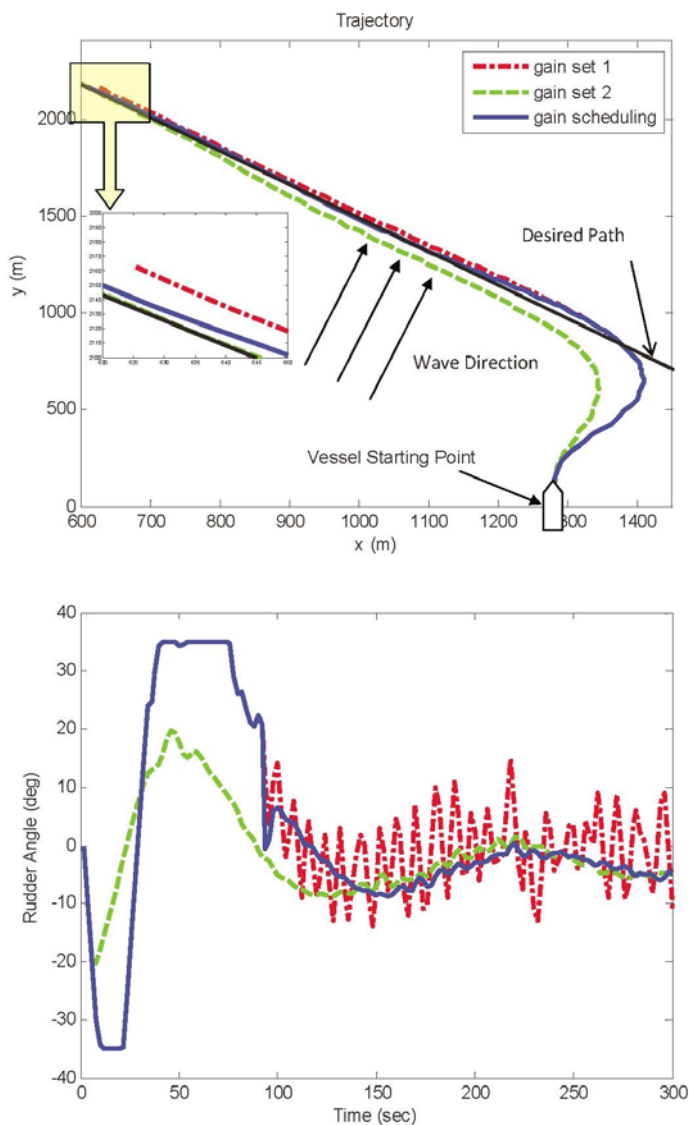


Figure 6. Simulation results of gain scheduling controller to reduce the steady state error and rudder oscillations.

Acknowledgements

This paper is the result of work sponsored by the Office of Naval Research through the Multidisciplinary University Research Initiative (MURI) under grants N00014-05-1-0537 and N00014-06-1-0879. This support is gratefully acknowledged. We also own many thanks to Professor Michael Parsons, Professor Okey Nwogu, James Wolfe and Rahul Subramanian for their work in second order wave drift force calculation, wave field generation and wave load calculation program.

References

- Amerongen, J.V. and H.R. van Nauta Lemke (1978). Optimum steering of ships with an adaptive autopilot. *Fifth ship Control Systems Symposium*.
- Amerongen, J.V. and H.R. van Nauta Lemke (1980). Criteria of optimum steering of ships. *Symposium on Ship Steering Automatic Control*.
- Breivik, M. and T.I. Fossen (2004a). Path following for marine surface vessels. *MTTS/IEEE TECHNO-OCEAN 4*, 2282–2289.
- Breivik, M. and T.I. Fossen (2004b). Path following of straight lines and circles for marine surface vessels. *Proceeding of the 6th IFAC CAMS*.
- Cao, Y. and T. Lee (2003). Maneuvering of surface vessels using a fuzzy logic controller. *Journal of Ship Research*, Vol 47, No. 2.
- Cao, Y., Z. Zhou and W. S. Vorus (2000). Application of a neural network predictor/controller to dynamic positioning of offshore structures. *Dynamic Positioning Conference*. Houston, Texas.
- Daidola, J.C. (1986). A simulation program for vessel's maneuvering at slow speeds. *Proceedings of Eleventh ship technology and research (star) symposium*.
- Do, K.D. and J. Pan (2003). Global tracking control of underactuated ships with off-diagonal terms. *Proceedings of the 42nd IEEE Conference on Decision and Control* pp. 1250–1255.
- Do, K.D. and J. Pan (2006). Underactuated ships follow smooth paths with integral actions and without velocity measurements for feedback: theory and experiments. *IEEE transactions on control systems technology* 14(2), 308–322.
- Do, K.D., Z.P. Jiang and J. Pan (2002). Underactuated ship global tracking under relaxed conditions. *IEEE Transactions on Automatic Control* 47, 1529–1536.
- Do, K.D., Z.P. Jiang and J. Pan (2004). Robust adaptive path following of underactuated ships. *Automatica* 40, 929–944.
- Dolinskaya, I.S., M. Kotinis, M.G. Parsons and R.L. Smith (2008). Optimal short-range routing of vessels in a seaway. Accepted by *Journal of Ship Research*.
- Encarnacao, P. and A. Pascoal (2001). Combined trajectory tracking and path following for marine vehicles. *Proceeding 9th Mediterranean Conference on Control and Automation*.
- English, J.W. and D.A. Wise (1975). Hydrodynamic aspects of dynamic positioning. *RINA*.
- Faltinsen, O.M. (1990). *Sea Loads on Ships and Offshore Structures*. Cambridge University Press.
- Fossen, T.I. (1994). *Guidance and Control of Ocean Vehicles*. John Wiley and Sons, Inc.
- Fossen, T.I., M. Breivik and R. Skjetne (2003). Line-of-sight path following of underactuated marine craft. *Proceeding of the Sixth*

- 1 *IFAC Conference Maneuvering and Control of Marine Crafts* pp.
2 244–249.
- 3 Jiang, Z.P. (2002). Global tracking control of underactuated ships by
4 Lyapunov's direct method. *Automatica* 38, 301–309.
- 5 Krstic, M., I. Kanellakopoulos and P.V. Kokotovic (1995). *Nonlinear
6 and Adaptive Control Design*. John Wiley and Sons, Inc.
- 7 Lapiere, L., D. Soetanto and A. Pascoal (2003). Nonlinear path
8 following with applications to the control of autonomous
9 underwater vehicles. *Proceeding 42nd IEEE Conference on
10 Decision and Control* 2, 1256–1261.
- 11 Lefeber, E., K.Y. Pettersen and H. Nijmeijer (2003). Tracking control
12 of an underactuated ship. *IEEE Transactions on Control Systems
13 Technology* 11, 52–61.
- 14 Lewis, E.V. (1989). *Principles of Naval Architecture*. Society of Naval
15 Architects and Marine Engineers.
- 16 Li, Z., J. Sun and S. Oh (2007). A robust nonlinear control design for
17 path following of a marine surface vessel. *IFAC Conference on
18 Control Applications in Marine Systems*.
- 19 Li, Z., J. Sun and S. Oh (2009). Design, analysis and experimental
20 validation of a robust nonlinear path following controller for
21 marine surface vessels. Accepted by *Automatica*.
- 22 Parsons M., A. C. Chubb and Y. Cao (1995). An assessment of fuzzy
23 logic vessel path control. *Journal of Oceanic Engineering*, Vol 20,
24 No. 4.
- 25 Perez, T., A. Ross and T.I. Fossen (2006). A 4-dof simulink model of a
26 coastal patrol vessel for manoeuvring in waves. *7th IFAC
27 Conference on Manoeuvring and Control of Marine Vessels
28 MCMC*.
- 29 Pettersen, K.Y. and E. Lefeber (2001). Way-point tracking control of
30 ships. *Proceeding of 40th IEEE Conference Decisions and Control*.
- 31 Pettersen, K.Y. and H. Nijmeijer (1998). Tracking control of an
32 underactuated surface vessels. *Proceeding of 37th IEEE Conference
33 Decisions and Control*.
- 34 Skjetne, R. and T. I. Fossen (2001). Nonlinear maneuvering and control
35 of ships. *Proceeding of the MTS/IEEE OCEANS*.
- 36 Skjetne, R., T. I. Fossen and P.V. Kokotovic (2004). Robust output
37 maneuvering for a class of nonlinear systems. *Automatica* 40,
38 373–383.
- 39 Velagic, J., Z. Vukic and E. Omerdic (2000). Adaptive fuzzy ship
40 autopilot for track-keeping. *IFAC Conference on Maneuvering
41 and Control of Marine Crafts*.
- 42 Vukic, Z., E. Omerdic and L. Kuljaca (1998). Improved fuzzy autopilot
43 for track-keeping. *IFAC Conference on Control Applications in
44 Marine Systems*.
- 45 Wolfe, J. (2007). Developing a ship motions prediction program using
46 linear theory for a ship maneuvering through a seaway. *Technical
47 Report*. Department of Naval Architecture and Marine
48 Engineering, University of Michigan, Ann Arbor.